

CHAPTER 2

Hydrologic Data Assimilation

Jeffrey P. Walker ¹ and Paul R. Houser ²

1. Department of Civil and Environmental Engg, The University of Melbourne, Australia
E-mail: j.walker@unimelb.edu.au

2. Hydrological Sciences Branch, NASA Goddard Space Flight Center, Greenbelt, USA
E-mail: paul.houser@nasa.gov

Key words: Data Assimilation; Quality Control; Validation; Dynamic Assimilation; Sequential Assimilation; Kalman Filter; Case Studies; Soil Moisture; Downscaling; Snow; Skin Temperature

2.1 Introduction

Earth observing satellites have revolutionised our understanding and prediction of the Earth system over the last 30 years, particularly in the meteorologic and oceanographic sciences. However, historically remote sensing data has not been widely used in hydrology. This can be attributed to: (i) a lack of dedicated hydrologic remote sensing instruments; (ii) inadequate retrieval algorithms for deriving global hydrologic information from remote sensing observations; (iii) a lack of suitable distributed hydrologic models for digesting remote sensing information; and (iv) an absence of techniques to objectively improve and constrain hydrologic model predictions using remote sensing data. Three ways that remote sensing observations have been used in distributed hydrologic models are: (i) as parametric input data, including soil and land cover properties; (ii) as initial condition data, such as initial snow water storage; and (iii) as time-varying hydrological state data, such as soil moisture content, to constrain model predictions. This chapter focuses on the latter.

The historic lack of hydrologic missions and observations has been the result of an emphasis on meteorologic and oceanographic missions and applications, due to the large scientific and operational communities that drive those fields. However, significant progress has been made over the past decade on defining hydrologically-relevant remote sensing observations through focused ground and airborne field studies. Gradually, satellite-based hydrologic data are becoming increasingly available, though little progress has been made in understanding their observation error. Land surface skin temperature and snow cover data have been available for many years, and satellite precipitation data are becoming available at increasing space and time resolutions. In addition, land cover and land use maps, vegetation parameters (albedo, leaf area index and greenness), and snow water equivalent data of increasing sophistication are becoming available from a number of sensors. Novel observations such as saturated fraction and changes in soil moisture, evapotranspiration, water level and velocity (i.e. runoff), and changes in total terrestrial water storage are also under development. Further, near-surface soil moisture, a parameter shown to play a critical role in weather, climate, agriculture, flood, and drought processes, is currently available from non-ideal sensor configuration observations. Moreover, two missions targeted at measuring near-

surface soil moisture with ideal sensor configuration are expected before the end of the decade.

Though remote sensing can make spatially comprehensive measurements of various components of the hydrologic system, it cannot provide information on the entire system, and the measurements represent only a snap shot in time. Land surface hydrology process models may be used to predict the temporal and spatial hydrologic system variations, but these predictions are often poor, due to model initialisation, parameter and forcing errors, and inadequate model physics and/or resolution. Figure 2.1 illustrates the hydrologic data assimilation challenge to optimally merge the spatially comprehensive but limited remote sensing observations with the comp

assimilatiofeer(e)-0.asim

wish to use both synergistically to obtain a more accurate result. Moreover, both contain different kinds of information, that when used together, provide an accuracy level that cannot be obtained when used individually.

For example, a hydrologic model provides both spatial and temporal near-surface and root zone soil moisture information at the model resolution, including errors resulting from inadequate model physics, parameters and forcing data. On the other hand, remote sensing observations contain near-surface soil moisture information at an instant in time, but do not give the temporal variation or the root zone moisture content. While the remote sensing observations can be used as initialisation input for models or as independent evaluation, providing we use a hydrologic model that has been adapted to use remote sensing data as input, we can use the hydrologic model predictions and remote sensing observations together to keep the simulation on track through data assimilation [Kostov and Jackson, 1993]. Moreover, large errors in near-surface soil moisture content prediction are unavoidable because of its highly dynamic nature. Thus when measured soil moisture data are available, their use to constrain the simulated data should improve the overall estimation of the soil moisture profile. However, this expectation is based on the assumption that measurement errors are smaller than simulation errors [Arya *et al.*, 1983].

Data assimilation techniques were pioneered by meteorologists [Daley, 1991] and have been used very successfully to improve operational weather forecasts for decades. Data assimilation has also been widely used in oceanography [Bennett, 1992] for improving ocean dynamics prediction. However, hydrologic data assimilation has just a few case studies demonstrating its utility. Fortunately, we have been able to jumpstart hydrologic data assimilation by building on knowledge derived from the meteorologic and oceanographic data assimilation experience, with significant advancements being made over the past decade.

One of the primary areas of hydrologic data assimilation application has been with soil moisture content. Other observation types, such as surface temperature, snow, terrestrial water storage and streamflow, have been used only in more recent applications. The study by Jackson *et al.* [1981] was among the first to update soil moisture predictions using near-surface soil moisture observations. In this application, the soil moisture values in both layers of the United States Department of Agriculture Hydrograph Laboratory model were substituted with observed near-surface soil moisture observations as they became available. The model's performance improvement was evaluated by annual runoff values. Ottlé and Vidal-Madjar [1994] used a similar approach but with the assimilation of thermal infrared derived near-surface soil moisture content.

Another early study based on the direct insertion assimilation method was that of Bernard *et al.* [1981]. Here synthetic observations of near-surface soil moisture content were used to specify the surface boundary condition of a classical one-dimensional soil water diffusion model, in order to estimate the surface flux. They found that large soil moisture content variations resulting from rainy periods required special handling of the upper boundary condition. Prevot *et al.* [1984] repeated this study with real observations and a similar approach was used by Bruckler and Witono [1989]. A more popular approach for the improved estimation of land surface fluxes has been the assimilation of screen-level measurements of relative humidity and temperature [Bouttier *et al.*, 1993; Viterbo and Beljaars, 1995]. To date only one study has explored the assimilation of remotely sensed land surface flux observations [Schuurmans *et al.*, 2003].

The first known study to use an “optimal” assimilation approach is that of Milly [1986]. In this study, a Kalman filter (a statistical assimilation approach) was used to update a simple linear reservoir model with near-surface soil moisture observations. It was not until

Entekhabi et al. [1994] that this approach was extended, when synthetically-derived vertical and horizontal polarised passive microwave and thermal infrared observations were assimilated into a one-dimensional soil moisture and temperature diffusion model using the Kalman filter. This synthetic study was further extended by *Walker et al.* [2001a] to more realistic observation times and *Walker et al.* [2001b] to a field application. Since then there has been a plethora of one-dimensional Kalman filter and variational assimilation studies.

Georgakakos and Baumer [1996] were one of the first to use the Kalman filter to update a hydrologic basin model with near-surface soil moisture measurements. Results showed that even when the observations carried substantial measurement errors, estimation of soil moisture profiles and total soil moisture storage was possible with an error that was smaller than that achieved without the use of remotely sensed data. *Walker et al.* [2002] were also among the first to use a three-dimensional Kalman filter based assimilation in a small catchment distributed hydrologic model. *Houser et al.* [1998] was the first detailed study of several alternative assimilation approaches, including direct insertion, statistical correction, Newtonian nudging and optimal interpolation. Both the Newtonian nudging and optimal interpolation approaches, pathological cases of the Kalman filter, showed the greatest improvement.

2.3 Summary of Data Assimilation

The data assimilation challenge is: given a (noisy) model of the system dynamics, find the best estimates of system states \mathbf{X} from (noisy) observations \mathbf{Z} . Most current approaches to this problem are derived from either the direct observer (i.e. Kalman filter) or dynamic observer (i.e. variational through time) techniques. Figure 2.3 illustrates schematically the key differences between these two approaches to data assimilation. To help the reader through the large amount of jargon typically associated with data assimilation, a list of terminology has been provided (Table 2.2).

Fig. 2.3

Table 2.2

2.3.1 Direct Observer Assimilation

The direct observer techniques sequentially update the model forecast, using the difference between observation \mathbf{Z} and model predicted observation $\hat{\mathbf{Z}}$, known as the ‘innovation’, whenever observations are available. The predicted observation is calculated from the model predicted or ‘background’ states, indicated by the superscript b . The correction added to the background state vector is the innovation multiplied by a weighting factor \mathbf{K} known as the ‘gain’ (sometimes called the Kalman gain). The gain represents the relative uncertainty in the observation and model variances, and is a number between 0 and 1 in the scalar situation. The resulting estimate of the state vector is known as the ‘analysis’, as indicated by the superscript a .

$$\hat{\mathbf{X}}_k^a = \mathbf{X}_k^b + \mathbf{K}(\mathbf{Z}_k - \hat{\mathbf{Z}}_k) \quad (2.1)$$

The subscript k refers to the time of the update. If the uncertainty of the predicted observation (as calculated from the background states and their uncertainty) is large relative to the uncertainty of the actual observation, then the analysis state vector takes on values that will yield the actual observation. Conversely, if the uncertainty of the predicted observation is

small relative to the uncertainty of the actual observation, then the analysis state vector is unchanged from the original background value. The commonly used direct observer methods are:

1. Direct Insertion
2. Statistical Correction
3. Successive Correction
4. Optimal Interpolation/Statistical Interpolation
5. Analysis Correction
6. Nudging
7. 3D Variational
8. Kalman Filter and variants

While approaches like direct insertion, nudging and optimal interpolation are computationally efficient and easy to implement, the updates do not account for observation uncertainty or utilise system dynamics in estimating model background state uncertainty, and information on estimation uncertainty is limited. The Kalman filter, while computationally demanding in its pure form, can be adapted for near-real-time application and provides information on estimation uncertainty. However, it has only limited capability to deal with model errors, and necessary linearisation approximations can lead to unstable solutions. The ensemble Kalman filter, while it can be computationally demanding (depending on the size of the ensemble) is well suited for near-real-time applications, is robust, very flexible and easy to use, and is able to accommodate a wide range of model error descriptions.

2.3.2 Dynamic Observer Assimilation

The dynamic observer techniques find the best fit between the forecast model state and the observations, subject to the initial state vector uncertainty Σ and observation uncertainty \mathbf{R} , by minimising over space and time an objective function J such as

$$J = \frac{1}{2}(\mathbf{X}_0 - \mathbf{X}_0^b)^T \Sigma_0^{b-1} (\mathbf{X}_0 - \mathbf{X}_0^b) + \frac{1}{2} \sum_0^{N-1} (\mathbf{Z}_k - \hat{\mathbf{Z}}_k)^T \mathbf{R}_k^{-1} (\mathbf{Z}_k - \hat{\mathbf{Z}}_k), \quad (2.2)$$

where the superscript b refers to the initial or ‘background’ estimate of the state vector, the subscript refers to time, and N is the number of time steps. To minimise the objective function over time, an assimilation time ‘window’ is defined and an ‘adjoint’ model is typically used to find the derivatives of the objective function with respect to the initial model state vector \mathbf{X}_0 . The adjoint is simply a mathematical operator that allows one to determine the sensitivity of the objective function to changes in the solution of the state equations by a single forward and backward pass over the assimilation window. While an adjoint is not strictly required (i.e. a number of forward passes can be used to numerically approximate the objective function derivatives with respect to each state), it makes the problem computationally tractable. The dynamic observer techniques can be considered simply as an optimisation or calibration problem, where the state vector – not the model parameters – at the beginning of each assimilation window is “calibrated” to the observations over that time period. The dynamic observer techniques can be formulated with:

1. Strong Constraint (variational)
2. Weak Constraint (dual variational or representer methods)

Strong constraint is where the model is assumed perfect, as in equation 2.2, while weak constraint is where errors in the model formulation are taken into account as process noise. This is achieved by including an additional term in equation 2.2 so that

$$J = \frac{1}{2}(\mathbf{X}_0 - \mathbf{X}_0^b)^T \Sigma_0^{b-1} (\mathbf{X}_0 - \mathbf{X}_0^b) + \frac{1}{2} \sum_0^{N-1} (\mathbf{Z}_k - \hat{\mathbf{Z}}_k)^T \mathbf{R}_k^{-1} (\mathbf{Z}_k - \hat{\mathbf{Z}}_k) + \frac{1}{2} \sum_0^{N-1} \mathbf{w}_k^T \mathbf{Q}_k^{-1} \mathbf{w}_k, \quad (2.3)$$

where \mathbf{w} is the model error vector and \mathbf{Q} is the model error variance-covariance matrix.

Dynamic observer methods are well suited for smoothing problems, but provide information on estimation accuracy only at considerable computational cost. Moreover, adjoints are not available for many existing hydrologic models, and the development of robust adjoint models is difficult due to the nonlinear nature of hydrologic processes.

2.3.3 Features of Data Assimilation

The potential benefit of data assimilation for hydrologic science is tremendous and can be summarised as follows [adapted from *Rood et al.*, 1994]:

- Organises the data by objectively interpolating from the observation space to the model space. The raw observations are organised and given dynamical consistency with the model equations, thereby enhancing their usefulness.
- Supplements the data by constraining the model's physical equations with parsimonious observations, which can be used to estimate unobserved quantities. This allows the progress of research that would be impossible without assimilation, because it allows for a more complete understanding of the true state of a hydrologic system (see Figure 2.4a).
- Complements the data by propagating information into regions of sparse observations using either observed spatial and temporal correlations, or the physical relationships included in the model (see Figure 2.4b).
- Quality controls the data through comparison of observations with previous forecasts to identify and eliminate spurious data. By performing this comparison repeatedly, it is possible to calibrate observing systems and identify biases or changes in observation system performance.
- Validates and improves the hydrological models by continuous model confrontation with real data. This helps to identify model weaknesses, such as systematic errors, and correct them.

Fig. 2.4 a, b

2.3.4 Quality Control for Data Assimilation

One of the major components of any data assimilation system is quality control of the input data stream. Quality control is a pre-assimilation rejection or correction of questionable or bad observations, which begins where the remote sensing product quality control activities leave off. The observation data from remote sensing systems contain errors that can be classified into two types:

1. Natural Error (including instrument and representativeness error)
2. Gross Error (including improperly calibrated instruments, incorrect registration or coding of observations, and telecommunication error)

These errors can be either random or spatially and/or temporally correlated with each other; inversion techniques and instrument biases can be correlated in time and space, and calibrations of remote sensing instruments can drift. To address these problems a number of quality control operations are performed.

The quality control process consists of a set of algorithms which examine each data item, individually or jointly, in the context of additional information. Their primary purpose is to determine which of the data are likely to contain unknown (incorrigible) gross errors, and which are not. Quality control proceeds in a three step process: (i) test for potential problem observations; (ii) attempt to correct the problem observation; and (iii) decide the fate of the observation (data rejection). The quality control algorithms can be categorised as follows:

- Quality control flags are used to check the data for inconsistencies noted during the measurement, transmission, pre/post processing and archiving stages.
- Consistency or sanity checks see if the observation absolute value or time rate of change is physically realistic. This check filters such things as observations outside the expected range, unit conversion problems, etc.
- Buddy checks compare the observation with comparable nearby (space and time) observations of the same type and reject the questioned observation if it exceeds a predefined level of difference.
- Background checks examine if the observation is changing similarly to the model prediction. If it is not, and the user has some reasonable confidence in the model, the observation may be questioned.

2.3.5 Validation Using Data Assimilation

The continuous confrontation of model predictions with observations in a data assimilation system presents a rich opportunity to better understand physical processes and observation quality in a structured, iterative, and open-ended learning process. Inconsistencies between observations and predictions are easily identified in a data assimilation system, providing a basis for observational quality control and validation. Systematic differences between observations and model predictions can identify systematic error. This methodology clearly illustrates the importance of a good quality forecast and an analysis that is reasonably faithful to the observations. If the hydrologic model makes reasonably good predictions, then the analysis must only make small changes to an accurate background field.

The validation of observations in a data assimilation system is centred on: (i) comparisons of new observations with the model forecast and the data assimilation analysis; and (ii) interpretation of the forecast error covariances. The data assimilation validation algorithms can be categorised as follows:

- Innovation evaluation compares the observation with the model prediction as either a single point in time or change over time; large or obvious deviations from the model prediction are probably wrong. Means, standard deviations, and time evolution of observed minus predicted fields are examined with the goal of detecting abrupt changes.
- Analysis residual evaluation compares the observation with the data assimilation analysis. Examination of the means, standard deviations, and time evolution of observed minus predicted fields will help to diagnose systematic or abrupt observation system changes. This technique is useful to diagnose the performance of the analysis,

and if the observations are being used effectively [Hollingsworth and Lonnberg, 1989].

- Observation withholding is a stringent method for validation in an assimilation system where some of the observational data are withheld from the analysis procedure in data-dense regions. This allows the analysis to be validated against the withheld observations.
- Error propagation is undertaken and changes in the regional distribution or absolute value of these errors could indicate observational problems.
- Model and observation bias is generally assumed to be zero and uncorrelated in space. These assumptions work reasonably well for *in situ* observations, but satellite observations are usually biased by inaccurate algorithms, and their errors are usually horizontally correlated because the same sensor is making all the observations. With recent work by Dee and Todling [2000] the bias of the model and observations can be continuously estimated and corrected for. Evaluation of these bias estimates in space and time may lead to additional insights on the observational characteristics.

2.4 Direct Observer Assimilation Methods

Land surface hydrology process models are typically nonlinear, and can be considered to forecast the system state vector \mathbf{X} at time $k+1$ as a function of the system state vector estimate at the previous time step k and a forcing vector \mathbf{U} . The model state forecast is subject to a model error vector \mathbf{w} , which represents errors in the model forcing data, initial conditions, parameters and physics. The state equation is given by

$$\mathbf{X}_{k+1} = a_k(\mathbf{X}_k, \mathbf{U}_k) + \mathbf{w}_k, \quad (2.4)$$

where a is a nonlinear operator. This equation can be linearised to obtain the ‘tangent linear model’ as

$$\mathbf{X}_{k+1} = \mathbf{A}_k \mathbf{X}_k + \mathbf{B}_k \mathbf{U}_k + \mathbf{w}_k. \quad (2.5)$$

The state space equation is subject to the initial state vector

$$\mathbf{X}_0 = \mathbf{X}(t_0) + \mathbf{e}_0, \quad (2.6)$$

with error vector \mathbf{e} . The observation equation is given by

$$\hat{\mathbf{Z}}_k = h_k(\mathbf{X}_k) + \mathbf{v}_k, \quad (2.7)$$

where h is a nonlinear operator. This equation can also be linearised as

$$\hat{\mathbf{Z}}_k = \mathbf{H} \mathbf{X}_k + \mathbf{Y}_k + \mathbf{v}_k, \quad (2.8)$$

with error vector \mathbf{v} .

The key assumptions of this assimilation approach are that the error terms \mathbf{w} , \mathbf{v} and \mathbf{e} are uncorrelated (white) through time and have Gaussian distributions as represented by their covariance matrices \mathbf{Q} , $\mathbf{\Sigma}$ and \mathbf{R} , respectively. That is

$$\begin{aligned} E(\mathbf{w}_k) &= 0 & E(\mathbf{w}_k \mathbf{w}_k^T) &= \mathbf{Q}_k \\ E(\mathbf{e}_0) &= 0 & E(\mathbf{e}_0 \mathbf{e}_0^T) &= \mathbf{\Sigma}_0^b, \\ E(\mathbf{v}_k) &= 0 & E(\mathbf{v}_k \mathbf{v}_k^T) &= \mathbf{R}_k \end{aligned} \quad (2.9)$$

where E is the expectation operator. The assumption that observation and model errors are unbiased relative to each other and the “truth” is the most restrictive assumption, most commonly violated assumption, and most detrimental assumption in terms of predictive performance.

One key question in the direct observer data assimilation technique, and the fundamental difference between the various methods, is the choice of the gain matrix \mathbf{K} . Ultimately \mathbf{K}_k should be chosen such that \mathbf{X}_k^a approaches the expectation of \mathbf{X}_k as k approaches infinity. This can be achieved by choosing \mathbf{K} as the optimal least squares estimator or Best Linear Unbiased Estimator (BLUE) analysis obtained as a solution to the variational optimisation problem posed in equation 2.2. That is, choosing \mathbf{K} such that objective function J is a minimum. This can be shown analytically to produce [Bouttier and Courtier, 1999]

$$\mathbf{K} = \mathbf{\Sigma}^b \mathbf{H}^T (\mathbf{H} \mathbf{\Sigma}^b \mathbf{H}^T + \mathbf{R})^{-1}, \quad (2.10)$$

where $\mathbf{H} \mathbf{\Sigma}^b \mathbf{H}^T = \hat{\mathbf{R}}$ is the covariance matrix of the predicted observation $\hat{\mathbf{Z}}$. Thus, on assimilation interval $k \in [0, N]$, the analysis \mathbf{X}_N^a given by the Kalman filter should be equal to the converged solution obtained by the adjoint method at time k equal to N .

From application of standard error propagation theory on the correction equation it can also be shown that the updated uncertainty of the states is given by

$$\mathbf{\Sigma}^a = (\mathbf{I} - \mathbf{K} \mathbf{H}) \mathbf{\Sigma}^b (\mathbf{I} - \mathbf{K} \mathbf{H})^T + \mathbf{K} \mathbf{R} \mathbf{K}^T, \quad (2.11)$$

where \mathbf{I} is the identity matrix. Equations 2.1, 2.5, 2.8, 2.10 and 2.11 form the basis of the Kalman filter approach [Kalman, 1960] to data assimilation.

Apart from the assumption that errors are unbiased and normally distributed, the difficulty associated with applying these equations is an estimate of the background variance-covariance matrix $\mathbf{\Sigma}^b$, and that to find the analysis \mathbf{X}^a one must compute $\mathbf{\Sigma}^b \mathbf{H}^T (\mathbf{H} \mathbf{\Sigma}^b \mathbf{H}^T + \mathbf{R})^{-1} (\mathbf{Z} - \hat{\mathbf{Z}}^b)$, which is computationally expensive. As a result, approximations to these equations and/or alternative methodologies of solving the key equations are sought. Ultimately, it is approximations to \mathbf{K} that are typically made.

2.4.1 Direct Insertion

One of the earliest and most simplistic approaches to data assimilation is direct insertion. As the name suggests, the forecast model states are directly replaced with the observations by essentially assuming that $\mathbf{K} = 1$. This approach makes the explicit assumption that the model is wrong (has no useful information) and that the observations are right, which both disregards important information provided by the model and preserves observation errors. A

further key disadvantage of this approach is that model physics are solely relied upon to propagate the information to unobserved parts of the system [Houser *et al.*, 1998; Walker *et al.*, 2001a].

2.4.2 Statistical Correction

A derivative of the direct insertion approach is the statistical correction approach, which adjusts the mean and variance of the model states to match those of the observations. This approach assumes the model pattern is correct but contains a non-uniform bias. First the predicted observations are scaled by the ratio of observation field standard deviation to predicted field standard deviation. Second, the scaled predicted observation field is given a block shift by the difference between the means of the predicted observation field and observation field [Houser *et al.*, 1998]. This approach also relies upon the model physics to propagate the information to unobserved parts of the system.

2.4.3 Successive Correction

This is an iterative type approach that uses weights \mathbf{W} to smooth observations into the model states, by modifying the states at all grid points within a specified radius of influence r of each observation s [Bratseth, 1986]. Any weighting system can be used, but the Cressman weights given by

$$W_{ij}^s = \begin{cases} \frac{r^2 - d_{ij}^2}{r^2 + d_{ij}^2} & d_{ij} < r \\ 0 & d_{ij} \geq r \end{cases} \quad (2.12)$$

are commonly used, where d_{ij} is the distance between grid point i,j and the observation. In practice the approach is usually applied consecutively to each observation s from 1 to s_f as

$$\mathbf{X}_k^{s+1} = \mathbf{X}_k^s + \mathbf{W}_k^s (\mathbf{Z}_k - \hat{\mathbf{Z}}_k), \quad (2.13)$$

and then setting $\mathbf{X}_k^a = \mathbf{X}_k^{s_f}$. This is equivalent to using $\mathbf{K}_k = \tilde{\mathbf{W}}^{s_f}$ in equation 2.1 where $\tilde{\mathbf{W}}^{s_f}$ is calculated from

$$\begin{aligned} \tilde{\mathbf{W}}^1 &= \mathbf{W}^1 \\ &\vdots \\ \tilde{\mathbf{W}}^{s+1} &= \mathbf{W}^{s+1} (\mathbf{I} + \mathbf{H} \tilde{\mathbf{W}}^s) + \tilde{\mathbf{W}}^s \\ &\vdots \end{aligned} \quad (2.14)$$

This approach assumes that the observations are more accurate than model forecasts, with the observations fitted as closely as is consistent. Moreover, it is ineffective in data sparse regions [Nichols, 2001].

2.4.4 Optimal Interpolation

The optimal interpolation (OI) approach, sometimes referred to as statistical interpolation, approximates the “optimal” solution from equation 2.10 by choosing

$$\mathbf{K} = \tilde{\Sigma}^b \mathbf{H}^T (\mathbf{H} \tilde{\Sigma}^b \mathbf{H}^T + \mathbf{R})^{-1} \quad (2.15)$$

where $\tilde{\Sigma}^b$ is an approximated background covariance matrix with a “fixed” structure for all time steps, and is often given by prescribed variances and a correlation function given only by distance [*Lorenc, 1981*].

2.4.5 Analysis Correction

This is a modification to the successive correction approach that is applied consecutively to each observation s from 1 to s_f as [*Lorenc et al., 1991*]

$$\mathbf{X}_k^{s+1} = \mathbf{X}_k^s + \mathbf{W}_k \mathbf{V}_k (\mathbf{Z}_k^s - \hat{\mathbf{Z}}_k), \quad (2.16)$$

where the observation vector \mathbf{Z}^s is also successively updated by

$$\mathbf{Z}_k^{s+1} = \mathbf{Z}_k^s - \mathbf{V}_k (\mathbf{Z}_k^s - \hat{\mathbf{Z}}_k), \quad (2.17)$$

and the weight matrices \mathbf{W} and \mathbf{V} given by

$$\mathbf{W}_k = \tilde{\Sigma}_k^b \mathbf{H}_k^T \mathbf{R}_k^{-1} \quad (2.18a)$$

$$\mathbf{V}_k = (\mathbf{I} + \mathbf{H}_k \mathbf{W}_k)^{-1}. \quad (2.18b)$$

In practice \mathbf{Z}^s is not updated and \mathbf{V}_k is approximated to avoid inversion. The result of these assumptions is an update equation equivalent to that for optimal interpolation [*Nichols, 1991*].

2.4.6 Nudging

The nudging approach approximates the gain matrix by the empirical function

$$\mathbf{K} \approx G(\mathbf{W}^T \mathbf{\Theta} \mathbf{W})(\mathbf{W} \mathbf{I})^{-1}, \quad (2.19)$$

where G is a nudging factor that gives the magnitude of the nudging term and has a value from 0 to 1, $\mathbf{\Theta}$ is an observational quality factor with a value from 0 to 1, \mathbf{I} is the identity matrix and \mathbf{W} is a temporal and spatial weighting function also with a value from 0 to 1. The function \mathbf{W} is given by $w_{xy}w_zw_t$, where w_{xy} is a horizontal weighting function (i.e. Cressman), w_z is a similar vertical weighting function, and w_t is a temporal weighting function. Each of these temporal/spatial weighting functions has a value from 0 to 1 [*Stauffer and Seaman, 1990*].

2.4.7 3D Variational

This approach directly solves the iterative minimisation problem given by equations 2.2 or 2.3 for $N = 1$ [*Parrish and Derber, 1992*]. The same approximation for the background covariance matrix as in the optimal interpolation approach is typically used. The solution gives an analysis which is similar in nature to the direct insertion approach.

2.4.8 Kalman Filter

The family of Kalman filter data assimilation approaches calculate the gain matrix in equation 2.10 by directly forecasting the background covariance matrix. In the traditional Kalman filter (KF) approach this is achieved by application of standard error propagation theory on the (tangent) linear model in equation 2.5. (The only difference between the Kalman filter and the extended Kalman filter is that the forecast model is linearised using a Taylor's series expansion; the same forecast and update equations are used for each.) The state covariance forecast equation is

$$\Sigma_{k+1}^b = \mathbf{A}_k \Sigma_k^b \mathbf{A}_k^T + \mathbf{Q}_k, \quad (2.20)$$

where \mathbf{A} is the linear operator from equation 2.5 and \mathbf{Q} is the model error covariance matrix given in equation 2.9. Thus, the (extended) Kalman filter requires propagation of the state covariances along with the states. While the approach gives an optimal analysis for the assumed statistics, the initial state error covariance matrix Σ_0 and more seriously the model error covariance matrix \mathbf{Q} are difficult to define, and often assumed ad hoc.

The standard extended Kalman filter (EKF) approach assumes an explicit model, which is limiting in terms of computational runtime as a result of the small step size necessary to satisfy stability criteria. However, it is also possible to apply the same update and state covariance forecast equations to an implicit formulation, such as the Crank-Nicholson scheme

$$\Phi_1 \mathbf{X}_{k+1} + \Omega_1 = \Phi_2 \mathbf{X}_k + \Omega_2, \quad (2.21)$$

by making the substitutions that

$$\mathbf{A}_k = \Phi_1^{-1} \Phi_2 \quad (2.22a)$$

$$\mathbf{B}_k \mathbf{U}_k = \Phi_1^{-1} [\Omega_2 - \Omega_1], \quad (2.22b)$$

but the inverse and multiplication required to calculate \mathbf{A} is costly for large systems [Walker *et al.*, 2001b].

The standard extended Kalman filter update and state covariance forecast equations can also be applied directly with a nonlinear state forecast model. This is achieved by numerically approximating the Jacobians \mathbf{A} and \mathbf{H} as required by

$$\mathbf{A}_k = \frac{\partial \mathbf{X}_{k+1}^b}{\partial \mathbf{X}_k^b} \quad (2.23a)$$

$$\mathbf{H}_k = \frac{\partial \mathbf{Z}_k}{\partial \mathbf{X}_k^b}. \quad (2.23b)$$

However, the cost of doing this is $n+1$ times the standard model run time, where n is the number of state variables to be updated by the assimilation. Note that only states with significant correlation to the observation need be included in the state covariance forecast and update [Walker and Houser, 2001].

A further approach to estimating the state covariance matrix is the ensemble Kalman filter (EnKF). As the name suggests, the covariances are calculated from an ensemble of state

forecasts using the Monte Carlo approach rather than a single discrete forecast of covariances. In this case m ensembles of n model predicted states \mathbf{X} are stored as \mathbf{x} using different initial conditions and forcing [Turner *et al.*, 2004], different parameters and/or models, different model error (additive/multiplicative/etc.), etc., in order to get a representative spread of state forecasts amongst the ensemble members. While this is quite straight forward, the question of what model error \mathbf{w} to apply, and how, is still a major unknown. Moreover, special care is required when m is less than the number of observations n .

Using this approach, the background state covariance matrix is basically calculated as

$$\mathbf{\Sigma}_k^b = \frac{(\mathbf{x}_k^b - \bar{\mathbf{x}}_k^b)(\mathbf{x}_k^b - \bar{\mathbf{x}}_k^b)^T}{m-1}. \quad (2.24)$$

This could then be used in equation 2.10 directly, except some smart maths is typically used so only matrices of size $(n \times m)$ are required [Evensen, 1994; Houtekamer and Mitchell, 1998]. Thus, $\mathbf{\Sigma}^b$ is never calculated explicitly. Here the analysis equation is presented as

$$\mathbf{X}_k^a = \mathbf{X}_k^b + \mathbf{B}_k^T \mathbf{b}_k, \quad (2.25)$$

where

$$\mathbf{B}_k^T = \mathbf{\Sigma}_k^b \mathbf{H}_k^T \quad (2.26a)$$

$$\mathbf{b}_k = (\mathbf{H}_k \mathbf{\Sigma}_k^b \mathbf{H}_k^T + \mathbf{R}_k)^{-1} (\mathbf{Z}_k - \hat{\mathbf{Z}}_k). \quad (2.26b)$$

By rearranging equation 2.26a and letting $\mathbf{y} = \mathbf{Z} + \boldsymbol{\zeta}$, where $\boldsymbol{\zeta}$ is a zero mean random observation error term with covariance matrix \mathbf{R} , \mathbf{b} is solved for each ensemble from

$$(\mathbf{H}_k \mathbf{\Sigma}_k^b \mathbf{H}_k^T + \mathbf{R}_k) \mathbf{b}_k = (\mathbf{y}_k - \hat{\mathbf{Z}}_k), \quad (2.27)$$

where

$$\mathbf{H}_k \mathbf{\Sigma}_k^b \mathbf{H}_k^T = \frac{\mathbf{q}_k \mathbf{q}_k^T}{m-1} \quad (2.28)$$

and

$$\mathbf{q}_k = \mathbf{H}_k (\mathbf{x}_k^b - \bar{\mathbf{x}}_k^b) = (\hat{\mathbf{z}}_k - \bar{\hat{\mathbf{z}}}_k). \quad (2.29)$$

The vector $\hat{\mathbf{z}}$ is the predicted observation vector for each of the respective ensemble members. In this case it is not necessary to solve for \mathbf{H} either, and the updates are made individually to each of the ensemble members. Finally, \mathbf{B} can be estimated from

$$\mathbf{B}_k^T = \frac{(\mathbf{x}_k^b - \bar{\mathbf{x}}_k^b)}{m-1} \mathbf{q}_k^T. \quad (2.30)$$

Reichle *et al.* [2001a] applied the ensemble Kalman filter to the soil moisture estimation problem and found it to perform as well as the numerical Jacobian approximation approach to

the extended Kalman filter, with the distinct advantage that the error covariance propagation is better behaved in the presence of large model nonlinearities. This was the case even when using only the same number of ensembles as required by the numerical approach to the extended Kalman filter i.e. $n+1$.

2.5 Dynamic Observer Assimilation Methods

In its pure form, the ‘variational’ (otherwise known as Gauss-Markov) dynamic observer assimilation methods use an adjoint to efficiently compute the derivatives of the objective function J with respect to each of the initial state vector values \mathbf{X}_0 . This adjoint approach is derived by defining the Lagrangian \mathcal{L} as the *adjoining* of the model to the model response using Lagrange multipliers $\boldsymbol{\lambda}$

$$\mathcal{L} = J + \sum_0^{N-1} \boldsymbol{\lambda}_{k+1}^T [\mathbf{X}_{k+1} - a_k(\mathbf{X}_k, \mathbf{U}_k)], \quad (2.31)$$

where ideally the second term is zero. Thus the Lagrange multiplier is chosen such that $\nabla \mathcal{L} = 0$ and $\boldsymbol{\lambda}_N = 0$, yielding (i.e. backward pass)

$$\boldsymbol{\lambda}_k = \mathbf{A}_k^T \boldsymbol{\lambda}_{k+1} - \mathbf{H}_k^T \mathbf{R}_k^{-1} (\mathbf{Z}_k - \hat{\mathbf{Z}}_k). \quad (2.32)$$

The derivative of the objective function is given from the Lagrange multiplier at time zero by $-\boldsymbol{\lambda}_0^T$ [Castelli *et al.*, 1999; Reichle *et al.*, 2001a]. Note that \mathbf{A}^T , the adjoint operator, is from the tangent linear model in equation 2.5, and effectively needs to be saved during the forward pass [Bouttier and Courtier, 1999]. Solution to the variational problem is then achieved by minimisation and iteration. In practical application the number of iterations is usually constrained to a small amount.

While ‘adjoint compilers’ are available (see <http://www.autodiff.com/tamc/>) for automatic conversion of the nonlinear forecast model into a tangent linear model, application of these is not straight forward. It is best to derive the adjoint at the same time as the model is developed.

2.6 Case Studies

Significant advances in hydrologic data assimilation have been made over the past decade from which we have selected a few case studies to demonstrate the utility of hydrologic data assimilation.

2.6.1 Case Study 1: Soil Moisture Assimilation

A one-dimensional Kalman filter soil moisture assimilation strategy was developed by Walker and Houser [2001] that provides a framework to constrain model predicted soil moisture with observations, using covariances that represent their respective uncertainty. A one-dimensional extended Kalman filter was used because of its computational efficiency and the fact that horizontal correlations between soil moisture prognostic variables of adjacent catchments at the scales of interest to climate modelling are likely only through the large-scale correlation of atmospheric forcing. A set of numerical experiments was undertaken for North America to illustrate the effectiveness of the Kalman filter assimilation scheme in

providing an accurate soil moisture estimate. When assimilating surface soil moisture once every 3 days, the scheme was generally able to retrieve the “true” profile soil moisture after only 1 month, and the predicted evapotranspiration and runoff fluxes were significantly improved.

Walker and Houser [2004] used this same EKF framework to address soil moisture satellite mission accuracy, repeat time and spatial resolution requirements through a numerical twin study. Simulated soil moisture profile retrievals were made by assimilating near-surface soil moisture observations with various accuracy, repeat time and spatial resolution. It was found that: (i) near-surface soil moisture observation error must be less than the model forecast error required for a specific application and must be better than 5%v/v accurate to positively impact soil moisture forecasts, (ii) daily near-surface soil moisture observations achieved the best soil moisture and evapotranspiration forecasts, (iii) near-surface soil moisture observations should have a spatial resolution of around half the model resolution, and (iv) satisfying the spatial resolution and accuracy requirements was much more important than repeat time. This kind of study is important for planning future observation systems, but it must be recognised that observation requirements are also highly application specific; for example, flood forecasting and precision agriculture requirements will likely have different requirements than climate modelling and policy planning, as they operate at different scales.

Walker and Houser [2002] was the first known study to use space-borne measurements of near-surface soil moisture content to estimate the spatial and temporal variation of soil moisture content at the continent scale by the process of data assimilation. Near-surface soil moisture measurements from the 6.6 GHz (C-band) channels of the Scanning Multi-channel Microwave Radiometer (SMMR) were assimilated into a land surface model over North America using a Kalman filter to correct for soil moisture estimation errors. Comparison with the limited ground-based point measurements of soil moisture content found a net improvement when near-surface soil moisture observations were assimilated. *Walker et al.* [2003] used a similar approach to estimate the spatial and temporal variation of soil moisture content across Australia (Figure 2.2). Unfortunately the lack of appropriate soil moisture evaluation data and mismatch in scale between model output and available data made it difficult to draw any conclusive statements regarding improvements in soil moisture predictions. There was however an obvious increase in correlation between soil moisture predictions and NDVI data when SMMR surface soil moisture data were assimilated. This provides some encouragement for pursuing assimilation experiments using the new AMSR-E data, and the collection of more appropriate ground-based soil moisture data for validation purposes.

2.6.2 Case Study 2: Downscaling With Data Assimilation

In a data assimilation framework, it may be possible to effectively increase the resolution of observations by making use of forecasts that include higher resolution meteorological, land cover, and soil texture information. Figure 2.5 demonstrates how low resolution brightness temperature observations have been used to estimate soil moisture at high resolution through variational assimilation into a land surface model [*Reichle et al.*, 2001b]. Spatial structures at scales well below the scale of the observations were resolved satisfactorily. This means that brightness images with a resolution of a few tens of kilometres are useful, even if the estimation scale of interest is of the order of a few kilometres, provided that fine-scale information is available on the meteorological forcing, land cover, and texture.

Fig. 2.5

The downscaling properties of data assimilation may also be able to help overcome the limitations of passive radiometric remote sensing (higher accuracy but lower spatial resolution) and active radar remote sensing (higher spatial resolution but lower accuracy) for sensing soil moisture. *Zhan et al.* [2004] tested this hypothesis by conducting an Observation System Simulation Experiment (OSSE), where the feasibility of retrieving surface soil moisture at a medium spatial scale (10 km) from both coarse scale (40 km) radiometer brightness temperature and fine scale (3 km) radar backscatter cross-section observations was evaluated using the extended Kalman filter. In this case the background field was an inversion of the passive data. Compared with the results from traditional soil moisture inversion algorithms, the combined active-passive extended Kalman filter retrieval algorithm significantly reduced soil moisture error at the medium scale. There is the potential to further enhance this downscaling approach by additionally using the information contained in overlapping observations.

2.6.3 Case Study 3: Snow Assimilation

Because of snow's high albedo, thermal properties, feedback to the atmosphere and being a medium-term water store, improved snow state estimation has the potential to greatly increase climatological and hydrological prediction accuracy. An analysis scheme to assimilate observed snow water equivalent into a land surface model has been developed [*Sun et al.*, 2004]. Using a set of numerical 'twin' experiments, the scheme is shown to be successful in retrieving the snow states (snow water equivalent, snow depth and snow temperature) from observations of snow water equivalent alone. The study illustrates that by assimilating remotely sensed snow water equivalent observations, the errors in forecast snow states from poor initial conditions can be removed (Figure 2.6), and the prediction of runoff and atmospheric fluxes improved. A comparison between monthly-averaged runoff and atmospheric fluxes showed negligible differences between the assimilation and truth simulations. Moreover, the assimilation significantly improved both upward shortwave and longwave radiation, and runoff predictions, as compared to no assimilation.

Fig. 2.6

Snow has several properties that make it uniquely challenging to assimilate, as follows. First, snow cover and depth observations provide an incomplete description of the multi-layer snow water equivalent, temperature and density states used in most physical snow models. For example, snow cover observations provide a binary snow presence description without snow quantity information. This is generally incompatible with data assimilation schemes that act on snow states. *Rodell et al.* [2002] overcame this problem by adding an arbitrarily thin layer of snow to model elements that have no snow when snow cover was observed. Second, snow is a highly transient model state that disappears and is not predicted for long periods of time during the year. This is generally incompatible with modern data assimilation techniques that seek to propagate error covariances; when there is no snow state prediction (i.e. when the temperature is above freezing), then there can also be no error propagation. This problem was overcome by *Sun et al.*, [2004] by simply reinitializing the error covariances when snow reappeared, but may not be so easily overcome in an ensemble Kalman filter context where ensemble members may vary significantly. Finally, in the presence of temperature bias, snow assimilation may have an undesirable water budget impact. *Cosgrove et al.* [2004] show that large water balance errors occur when imperfect snow melting processes interact with the direct insertion of perfect snow observations. Constraining these snow melt biases is important for achieving optimal assimilation results, and is an important topic for future research.

2.6.4 Case Study 4: Skin Temperature Assimilation

The land surface skin temperature state is a principle control on land-atmosphere fluxes of water and energy. It is closely related to soil water states, and is easily observable from space and aircraft infrared sensors in cloud-free conditions. The usefulness of skin temperature in land data assimilation studies is limited by its very short memory (on the order of minutes) due to the very small heat storage it represents. *Radakovich et al.* [2001] have demonstrated skin temperature data assimilation in a land surface model (Figure 2.7) using three-hourly observations from the International Satellite Cloud Climatology Project (ISCCP). Incremental and semi-diurnal bias correction techniques based on *Dee and da Silva* [1998] were developed to account for biased skin temperature forecasts. The assimilation of ISCCP-derived surface skin temperature significantly reduced the bias and standard deviation between model predictions and the NCEP reanalysis [*Kalnay et al.*, 1996]. However, the assimilation of ISCCP-derived surface skin temperature has a substantial impact on the sensible heat flux, due to an enhanced gradient between the surface and 2m air temperatures. If the near-surface air temperature were interactive, as in a coupled land-atmosphere model, then it would respond to this enhanced flux rather than maintaining the artificial temperature gradient.

Fig. 2.7

2.7 Summary

Hydrologic data assimilation is an objective method to estimate the hydrologic system states from irregularly distributed observations. These methods integrate observations into numerical prediction models to develop physically consistent estimates that better describe the hydrologic system state than the raw observations alone. This process is extremely valuable for providing initial conditions for hydrologic system prediction and/or correcting hydrologic system prediction, and for increasing our understanding and improving parameterisation of hydrologic system behaviour through various diagnostic research studies.

Hydrologic data assimilation is still in its infancy, with many open areas of research. Development of hydrologic data assimilation theory and methods is needed to: (i) better quantify and use model and observation errors; (ii) create model independent data assimilation algorithms that can account for the typical non-linear nature of hydrologic models; (iii) optimise data assimilation computational efficiency for use in large operational hydrological applications; (iv) use forward models to enable the assimilation of remote sensing radiances directly; (v) link model calibration and data assimilation to optimally use available observation information; (vi) create multivariate hydrologic assimilation methods to use multiple observations with complementary information; (vii) quantify the potential of data assimilation downscaling; and (viii) create methods to extract the primary information content from observations with redundant or overlaying information. Further, the regular provision of snow, soil moisture, and surface temperature observations with improved knowledge of observation errors in time and space are essential to advance hydrologic data assimilation. Hydrologic models must also be improved to: (i) provide more “observable” land model states, parameters, and fluxes; (ii) include advanced processes such as river runoff and routing, vegetation and carbon dynamics, and groundwater interaction to enable the assimilation of emerging remote sensing products; (iii) have valid and easily updated adjoints, and (iv) have knowledge of their prediction errors in time and space. The assimilation of additional types of hydrologic observations, such as streamflow, vegetation dynamics, evapotranspiration, and groundwater or total water storage must be developed.

As with most current data assimilation efforts, we describe data assimilation procedures that are implemented in uncoupled models. However, it is well known that the high-resolution time and space complexity of hydrologic phenomena have significant interaction with atmospheric, biogeochemical, and oceanic processes. Scale truncation errors, unrealistic physics formulations, and inadequate coupling between hydrology and the overlying atmosphere can feedback to cause serious systematic hydrologic errors. Hydrologic balances cannot be adequately described by current uncoupled hydrologic data systems, because large analysis increments that compensate for errors in coupling processes (e.g. precipitation) result in important non-physical contributions to the energy and water budgets. Improved coupled process models with improved feedback processes, better observations, and comprehensive methods for coupled assimilation are needed to achieve the goal of fully coupled data assimilation systems that should produce the best and most physically consistent estimates of the Earth system.

2.8 References

- Arya, L. M., Richter, J. C., and Paris, J. F., (1983). Estimating profile water storage from surface zone soil moisture measurements under bare field conditions. *Wat. Resour. Res.*, **19**(2): 403-412.
- Bennett, A. F., (1992.) *Inverse methods in physical oceanography*. Cambridge University Press, 346 pp.
- Bernard, R., Vauclin, M., and Vidal-Madjar, D., (1981). Possible use of active microwave remote sensing data for prediction of regional evaporation by numerical simulation of soil water movement in the unsaturated zone. *Wat. Resour. Res.*, **17**(6): 1603-1610.
- Bouttier, F., and Courtier P., (1999). *Data assimilation concepts and methods*. ECMWF training course notes.
- Bouttier, F., Mahfouf, J. -F., and Noilhan, J., (1993). Sequential assimilation of soil moisture from atmospheric low-level parameters. Part I: Sensitivity and calibration studies, *J. Appl. Meteorol.*, **32**(8): 1335-1351.
- Bratseth, A. M., (1986). Statistical interpolation by means of successive corrections. *Tellus* **38A**: 439-447.
- Bruckler, L., and Witono, H. (1989). Use of remotely sensed soil moisture content as boundary conditions in soil-atmosphere water transport modeling: 2. Estimating soil water balance. *Wat. Resour. Res.*, **25**(12): 2437-2447.
- Castelli, F., Entekhabi, D., and Caporali, E., (1999). Estimation of surface heat flux and an index of soil moisture using adjoint-state surface energy balance. *Wat. Resour. Res.*, **35**(10): 3115-3125.
- Charney, J. G., Halem, M., and Jastrow, R., (1969). Use of incomplete historical data to infer the present state of the atmosphere. *J. Atmos. Sci.* **26**: 1160-1163.
- Cosgrove, B. A., Houser P. R., and Toll D. L., (2004). Impact of surface forcing biases on snow assimilation. *In preparation*.
- Daley, R., (1991). *Atmospheric data analysis*. Cambridge University Press, 460 pp.
- Dee, D. P., and da Silva, A., (1998). Data assimilation in the presence of forecast bias. *Q. J. R. Meteorol. Soc.*, **124**: 269-295.

- Dee, D. P., and Todling, R., (2000). Data assimilation in the presence of forecast bias: The GEOS moisture analysis. *Mon. Wea. Rev.*, **128**: 3268-3282.
- Entekhabi, D., Nakamura H., and Njoku, E. G., (1994). Solving the inverse problem for soil moisture and temperature profiles by sequential assimilation of multifrequency remotely sensed observations. *IEEE Trans. Geosci. Rem. Sens.*, **32**: 438-448.
- Evensen, G., (1994). Sequential data assimilation with a nonlinear quasi-geostrophic model using Monte Carlo methods to forecast error statistics. *J. Geophys. Res.*, **99**(C5): 10143-10162.
- Georgakakos, K. P., and Baumer, O. W., (1996). Measurement and utilization of on-site soil moisture data. *J. Hydrol.*, **184**: 131-152.
- Hollingsworth, A. and Lonnberg, P., (1989). The verification of objective analyses: Diagnostics of analysis system performance. *Meteor. Atmos. Phys.*, **40**: 3-27.
- Houser, P. R., et al., (1998). Integration of soil moisture remote sensing and hydrologic modeling using data assimilation. *Wat. Resour. Res.*, **34**(12): 3405-3420.
- Houtekamer, P. L., and Mitchell, H. L., (1998). Data assimilation using a Ensemble Kalman filter techniques, *Mon. Weather Rev.*, **126**: 796-811.
- Jackson, T. J., et al., (1981). Soil moisture updating and microwave remote sensing for hydrological simulation. *Hydrol. Sci. B.*, **26**(3): 305-319.
- Kalman, R. E., (1960). A new approach to linear filtering and prediction problems. *Trans. ASME, Ser. D, J. Basic Eng.* **82**: 35-45.
- Kalnay, E., et al., (1996) The NCEP/NCAR 40-year reanalysis project. *Bullet. Amer. Meteorol. Soc.*, **77**: 437-471.
- Kostov, K. G., and Jackson, T. J., (1993). Estimating profile soil moisture from surface layer measurements – A review. In: *Proc. The International Society for Optical Engineering*, Vol. 1941, Orlando, Florida, 125-136.
- Lorenc, A., (1981). A global three-dimensional multivariate statistical interpolation scheme. *Mon. Wea. Rev.*, **109**: 701-721.
- Lorenc, A. C., Bell, R. S., and Macpherson, B. (1991). The Meteorological Office analysis correction data assimilation scheme. *Quart. J. Roy. Meteor. Soc.*, **117**, 59-89
- Milly, P. C. D., (1986). Integrated remote sensing modelling of soil moisture: sampling frequency, response time, and accuracy of estimates. *Integrated Design of Hydrological Networks - Proceedings of the Budapest Symposium*, **158**: 201-211.
- Nichols, N. K., (2001). *State estimation using measured data in dynamic system models*, Lecture notes for the Oxford/RAL Spring School in Quantitative Earth Observation.
- Ottlé, C., and Vidal-Madjar, D., (1994). Assimilation of soil moisture inferred from infrared remote sensing in a hydrological model over the HAPEX-MOBILHY Region. *J. Hydrol.*, **158**: 241-264.
- Parish, D., and Derber, J., (1992). The National Meteorological Center's spectral statistical interpolation analysis system. *Mon. Wea. Rev.*, **120**: 1747-1763.
- Prevot, L., et al., (1984). Evaporation from a bare soil evaluated using a soil water transfer model and remotely sensed surface soil moisture data. *Wat. Resour. Res.*, **20**(2): 311-316.

- Radakovich, J. D., Houser, P. R., da Silva, A., and Bosilovich, M. G., (2001). Results from global land-surface data assimilation methods. *Proceedings AMS 5th Symposium on Integrated Observing Systems*, Albuquerque, NM, 14-19 January, 132-134.
- Reichle, R. H., and McLaughlin, D. B., (2001a). Variational data assimilation of microwave radiobrightness observations for land surface hydrologic applications. *IEEE Trans. Geosci. Rem. Sens.*, **39**(8): 1708-1718.
- Reichle, R. H., Entekhabi, D., and McLaughlin, D. B., (2001b). Downscaling of radiobrightness measurements for soil moisture estimation: A four-dimensional variational data assimilation approach, *Wat. Resour. Res.*, **37**(9): 2353-2364.
- Rodell, M., (2002). Use of MODIS-derived snow fields in the Global Land Data Assimilation System. *Proceedings GAPP Mississippi River Climate and Hydrology Conference*, New Orleans.
- Rood, R. B., Cohn, S. E., and Coy, L., (1994.) Data assimilation for EOS: The value of assimilated data, Part 1. *The Earth Observer*, **6**(1): 23-25.
- Schuermans, J. M., et al., (2003). Assimilation of remotely sensed latent heat flux in a distributed hydrological model. *Adv. Water Resour.*, **26**(2): 151-159.
- Stauffer, D. R., and Seaman, N. L., (1990). Use of four-dimensional data assimilation in a limited-area mesoscale model. Part I: Experiments with synoptic-scale data. *Mon. Wea. Rev.*, **118**: 1250-1277.
- Sun, C., Walker, J. P., and Houser, P. R., (2004). A methodology for snow data assimilation in a land surface model. *J. Geophys. Res.-Atmos.*, **109**.
- Turner, M. R. J., Walker, J. P., and Oke, P. R., (2004). Ensemble member generation for sequential data assimilation. *In preparation*.
- Viterbo, P., and Beljaars, A., (1995). An improved land surface parameterization scheme in the ECMWF model and its validation. *J. Climate*, **8**: 2716-2748.
- Walker J. P., and Houser, P. R., (2001). A methodology for initialising soil moisture in a global climate model: assimilation of near-surface soil moisture observations, *J. Geophys. Res.-Atmos.*, **106**(D11): 11761-11774.
- Walker, J. P., Willgoose, G. R., and Kalma, J. D., (2001a). One-dimensional soil moisture profile retrieval by assimilation of near-surface observations: A comparison of retrieval algorithms. *Adv. Water Resour.*, **24**(6): 631-650.
- Walker, J. P., Willgoose, G. R. and Kalma, J. D., (2001b). One-dimensional soil moisture profile retrieval by assimilation of near-surface measurements: A simplified soil moisture model and field application. *J. Hydromet.*, **2**(4): 356-373.
- Walker, J. P., Willgoose, G. R. and Kalma, J. D., (2002). Three-dimensional soil moisture profile retrieval by assimilation of near-surface measurements: Simplified Kalman filter covariance forecasting and field application. *Wat. Resour. Res.*, **38**(12): 1301.
- Walker, J. P., and Houser, P. R., (2002). Soil moisture estimation using remote sensing. *Proceedings 27th Hydrology and Water Resources Symposium*. The Institute of Engineers Australia, Melbourne, Australia, 20 - 23 May.
- Walker, J. P., and Houser, P. R., (2004). Requirements of a global near-surface soil moisture satellite mission: Accuracy, repeat time, and spatial resolution. *Adv. Water Resour.*, **27**: 785-801.

- Walker, J. P., Ursino, N., Grayson, R. B., and Houser, P. R., (2003). Australian root zone soil moisture: Assimilation of remote sensing observations, In: D. Post (Ed.), *Proceedings of the International Congress on Modelling and Simulation (MODSIM)*. Modelling and Simulation Society of Australia and New Zealand, Inc., Townsville, Australia, 14-17 July, 1: 380-385.
- Zhan, X., et al., (2004). Retrieving medium resolution surface soil moisture from coarse resolution radiometer and fine resolution radar observations using the Kalman filter. *In preparation*.

Table 2.1: Characteristics of hydrologic observations potentially available within the next decade.

Hydrologic Quantity	Remote Sensing Technique	Time Scale	Space Scale	Accuracy Considerations	Example Sensors
Precipitation	Thermal infrared	Hourly 1day 15days	4km 1km 60m	Tropical convective clouds only	GOES MODIS, AVHRR Landsat, ASTER
	Passive microwave	3hour	10km	Land calibration problems	TRMM, SSMI, AMSR-E, GPM
	Active microwave	Daily	10m	Land calibration problems	TRMM, GPM
Surface soil moisture	Passive microwave	1-3days	25-50km	Limited to sparse vegetation, low topographic relief	AMSR-E, SMOS, Hydros
	Active microwave	3days 30days	3km 10m	Significant noise from vegetation and roughness	ERS, JERS, RadarSat
Surface skin temperature	Thermal infrared	1hour 1day 15days	4km 1km 60m	Soil/vegetation average, cloud contamination	GOES MODIS, AVHRR Landsat, ASTER
Snow cover	Visible/ thermal infrared	1hour 1day 15days	4km 500m-1km 30-60m	Cloud contamination, vegetation masking, bright soil problems	GOES MODIS, AVHRR Landsat, ASTER
Snow water equivalent	Passive microwave	1-3days	10km	Limited depth penetration	AMSR-E
	Active microwave	30days	100m	Limited spatial coverage	SnoSat or CLPP (proposed missions)
Water level/ velocity	Laser	10days	100m	Cloud penetration problems	ICESAT
	Radar	30days	1km	Limited to large rivers	TOPEX/POSEIDON
Total water storage changes	Gravity changes	30days	1000km	Bulk water storage change	GRACE
Evaporation	Thermal infrared	1hour 1day 15days	4km 1km 60m	Significant assumptions	GOES MODIS, AVHRR Landsat, ASTER

Table 2.2: Commonly used data assimilation terminology.

<i>State</i>	condition of a physical system ie. soil moisture
<i>Prognostic</i>	a model state required to propagate the model forward in time
<i>Diagnostic</i>	a model state/flux diagnosed from the prognostic states – not required to propagate the model
<i>Observation</i>	measurement of a model diagnostic or prognostic
<i>Covariance matrix</i>	describes the standard deviations & correlations
<i>Prediction</i>	model estimate of states or covariances
<i>Update</i>	correction to a model prediction using observations
<i>Background</i>	prediction prior to an update
<i>Analysis</i>	prediction after an update
<i>Innovation</i>	observation-prediction
<i>Gain matrix</i>	correction factor applied to the innovation
<i>Tangent linear model</i>	linearised (using Taylor's series expansion) version of a non-linear model
<i>Adjoint</i>	operator allowing the model to be run backwards in time

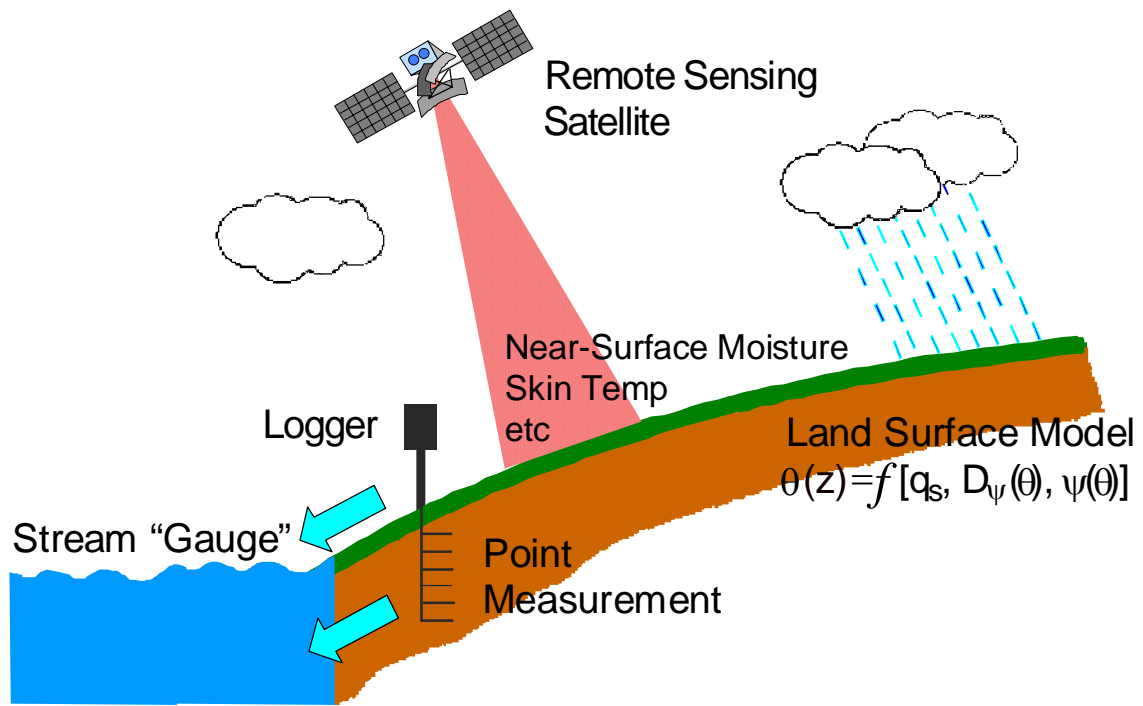


Figure 2.1: Schematic of the hydrologic data assimilation challenge.

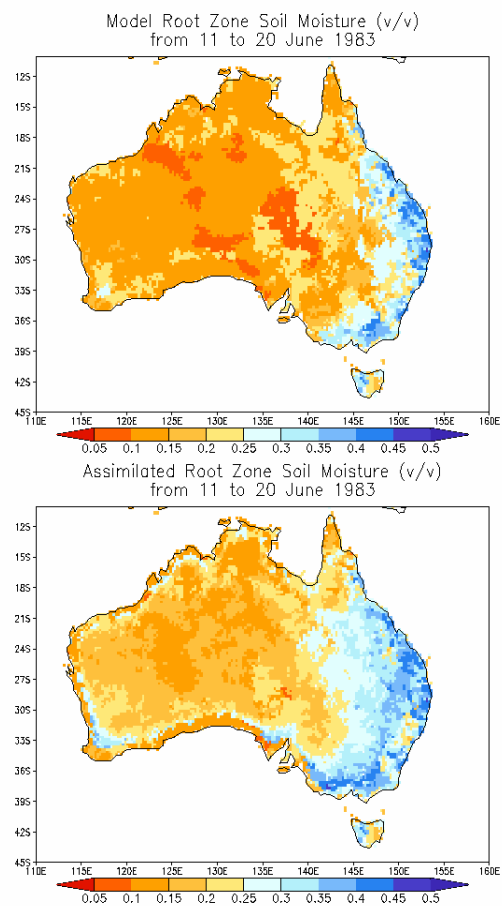
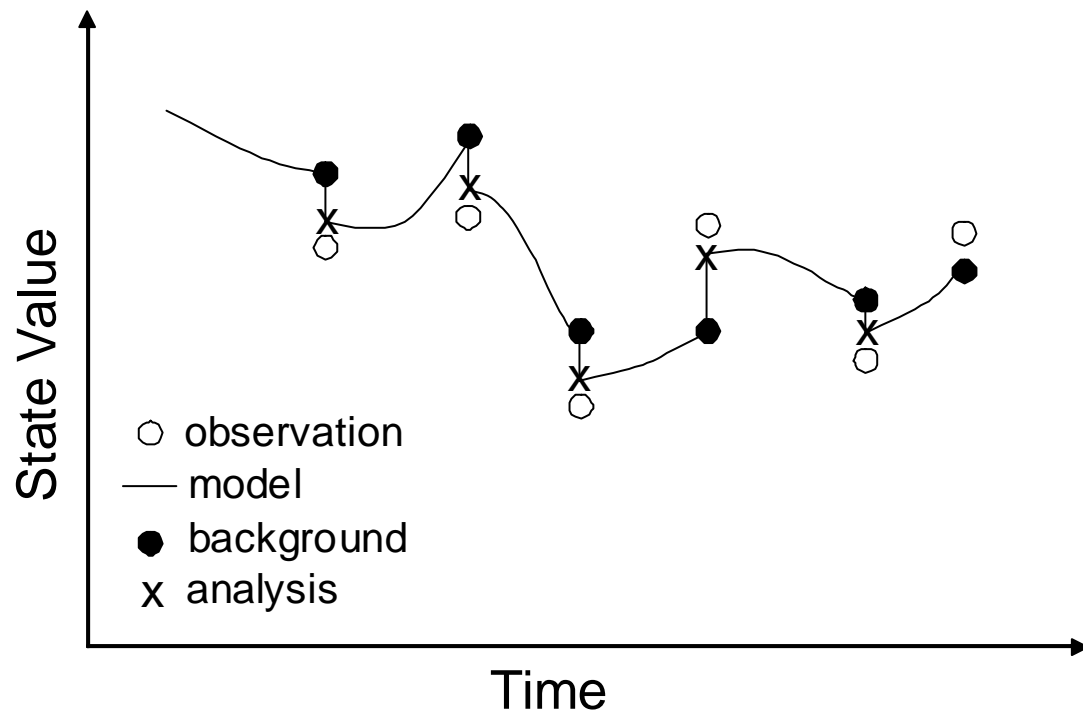
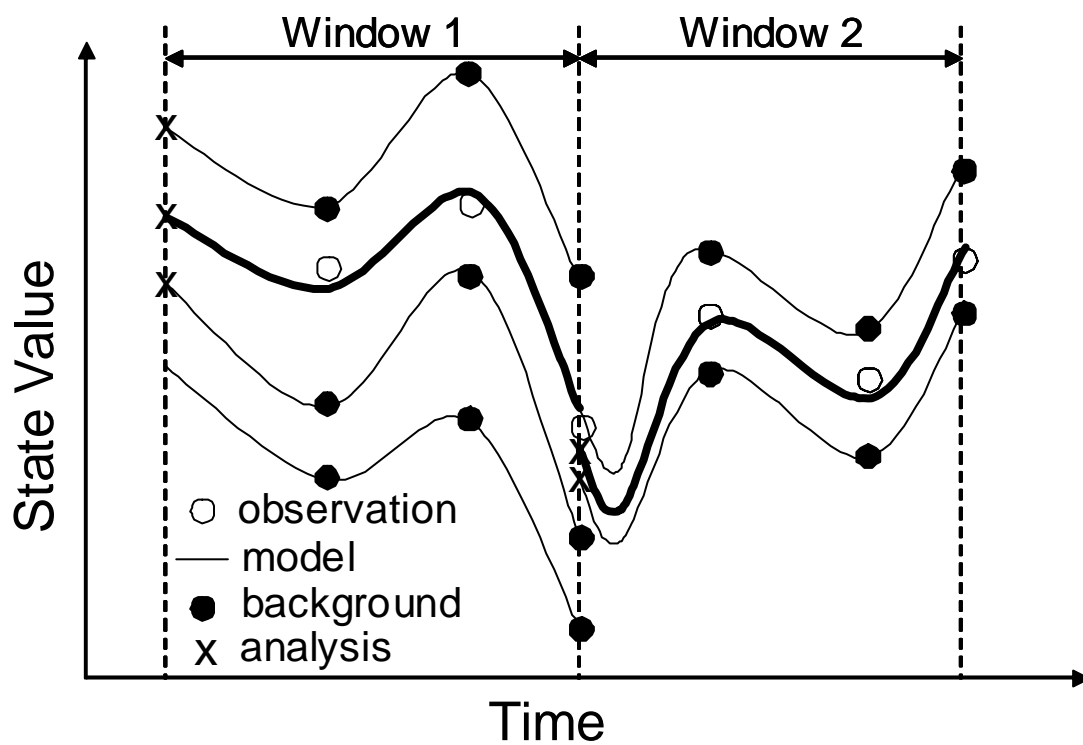


Figure 2.2: Satellite observations of near-surface soil moisture content made by the scanning multifrequency microwave radiometer (SMMR) are used to constrain hydrologic model predictions of soil moisture throughout the root zone using data assimilation.



a)



b)

Figure 2.3: Schematic of the a) direct observer and b) dynamic observer assimilation approaches.

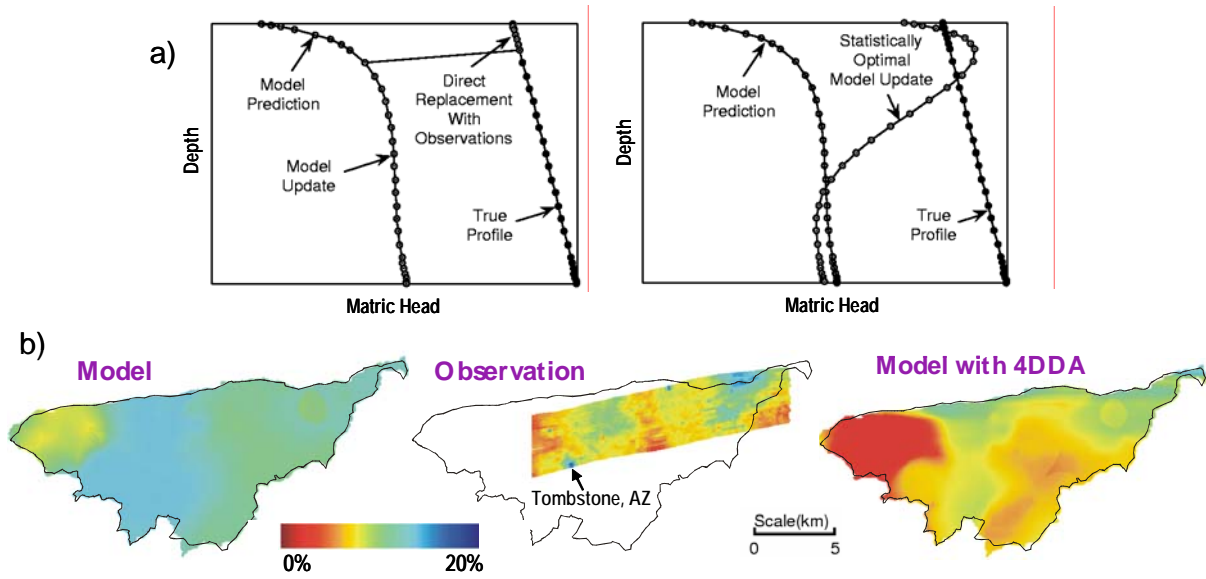


Figure 2.4: Example of how data assimilation supplements data and complements observations: (a) Numerical experiment results demonstrating how near-surface soil moisture measurements are used to retrieve the unobserved root zone soil moisture state using (left panel) direct insertion and (right panel) a statistical assimilation approach [Walker *et al.*, 2001a]; (b) Six Push Broom Microwave Radiometer (PBR) images gathered over the USDA-ARS Walnut Gulch Experimental Watershed in southeast Arizona were assimilated into the TOPLATS hydrological model using several alternative assimilation procedures [Houser *et al.*, 1998]. The observations were found to contain horizontal correlations with length scales of several tens of kilometres, thus allowing soil moisture information to be advected beyond the area of the observations.

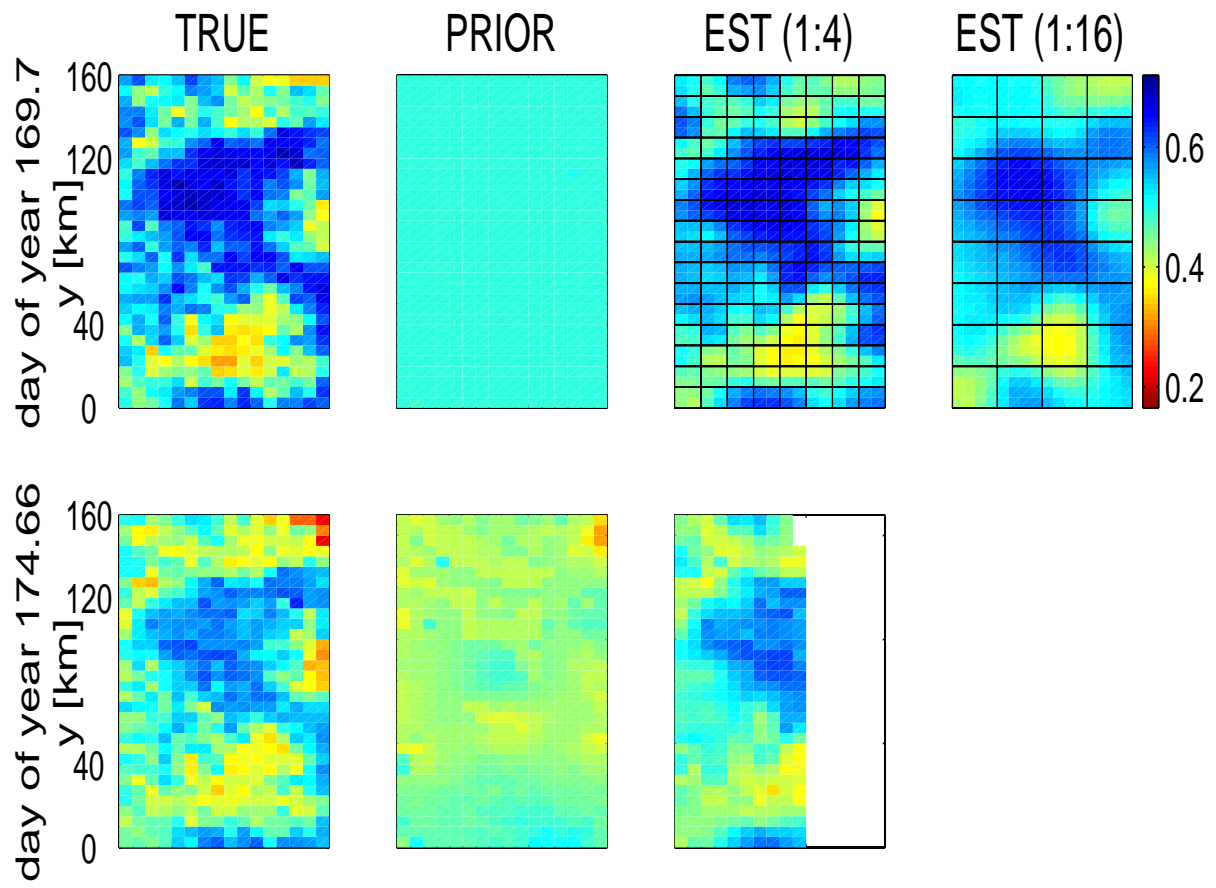


Figure 2.5: True and prior surface soil saturation (in the first two columns) at three different times. Corresponding estimates for downscaling ratios of (1:4) and (1:16) are shown in the third and fourth columns. The resolution of the observations used to compute the downscaled estimates are indicated with solid black grid lines [Reichle, 2001b].

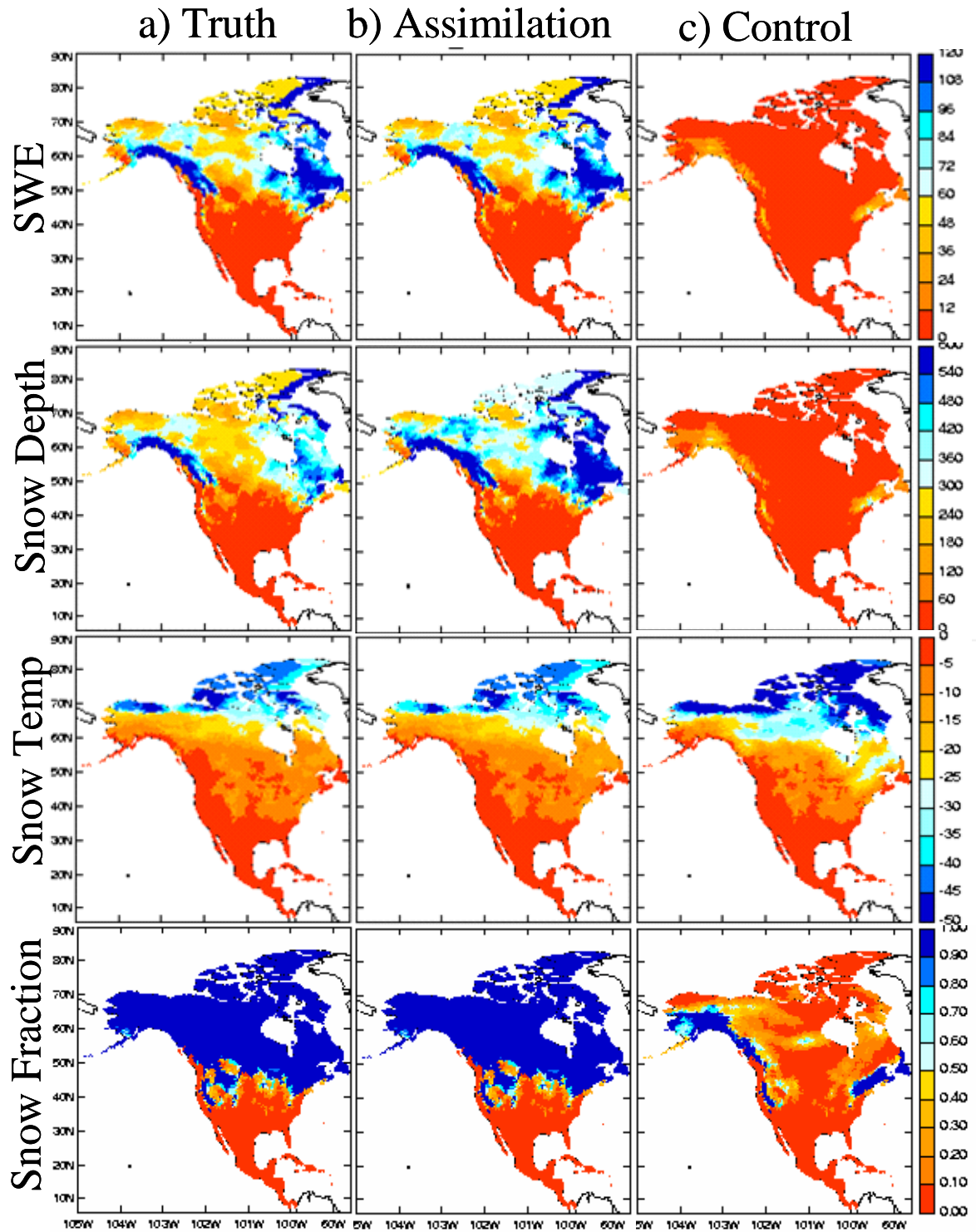


Figure 2.6: Comparison of snow simulations on January 5, 1987 over North America for snow water equivalent (in mm, top row); snow depth (in mm, second row); average snow temperature (in $^{\circ}\text{C}$, third row); and areal snow fraction (bottom row) from a) truth run (using spin up initial condition), b) assimilation run (with degraded initial condition and assimilation of daily total snow water equivalent observations), and c) control run (with degraded initial condition) [Sun *et al.*, 2004].

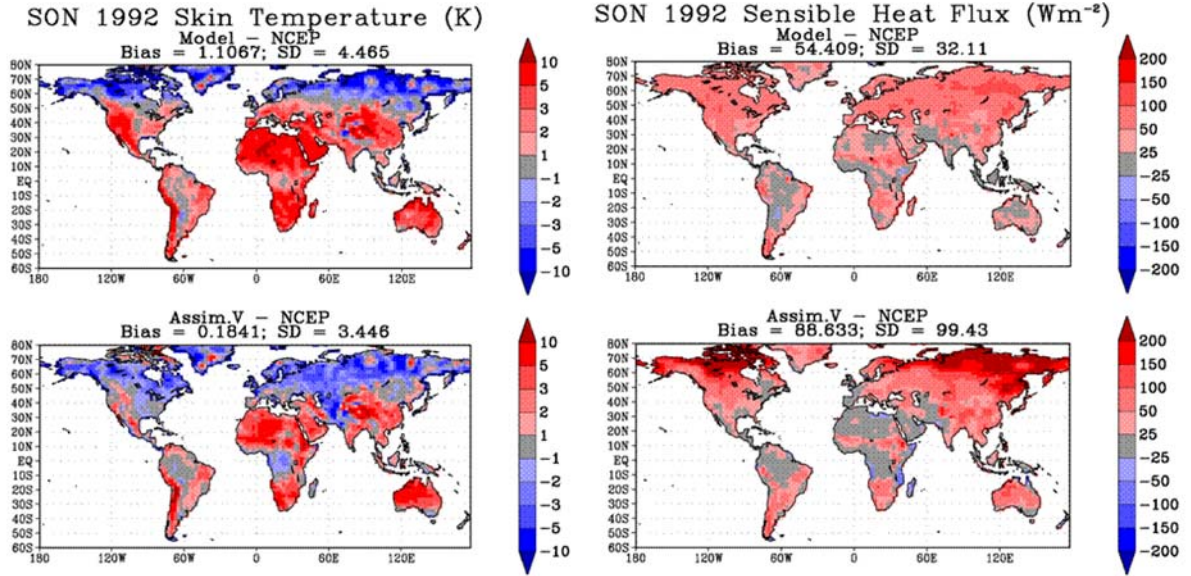


Figure 2.7: Differences between simulated and reanalysis (top left), assimilated and reanalysis (bottom left) mean skin temperature (K), and the resulting differences between simulated and reanalysis (top right), and assimilated and reanalysis (bottom right) mean sensible heat fluxes (Wm^{-2}) for September through November 1992. Global terrestrial mean bias and standard deviation (SD) for September through November are also noted [Radakovich *et al.*, 2001].